

COMMUNICATION

Denaturant-induced Expansion and Compaction of a Multi-domain Protein: IgG

Lin Guo^{1†}, Pramit Chowdhury^{1†}, Julie M. Glasscock² and Feng Gai^{1*}

¹Department of Chemistry,
University of Pennsylvania,
Philadelphia, PA 19104, USA

²Department of Biochemistry
and Molecular Biophysics,
School of Medicine, University
of Pennsylvania, Philadelphia,
PA 19104, USA

Received 12 November 2007;
received in revised form
26 February 2008;
accepted 5 March 2008
Available online
18 March 2008

It is generally believed that unfolded or denatured proteins show random-coil statistics and hence their radius of gyration simply scales with solvent quality (or concentration of denaturant). Indeed, nearly all proteins studied thus far have been shown to undergo a gradual and continuous expansion with increasing concentration of denaturant. Here, we use fluorescence correlation spectroscopy (FCS) to show that while protein A, a multi-domain and predominantly helical protein, expands gradually and continuously with increasing concentration of guanidine hydrochloride (GdnHCl), the F(ab')₂ fragment of goat anti-rabbit antibody IgG, a multi-subunit all β -sheet protein does not show such continuous expansion behavior. Instead, it first expands and then contracts with increasing concentration of GdnHCl. Even more striking is the fact that the hydrodynamic radius of the most expanded F(ab')₂ ensemble, observed at 3–4 M GdnHCl, is ~ 3.6 times that of the native protein. Further FCS measurements involving urea and NaCl show that the unusually expanded F(ab')₂ conformations might be due to electrostatic repulsions. Taken together, these results suggest that specific interactions need to be considered while assessing the conformational and statistical properties of unfolded proteins, particularly under conditions of low solvent quality.

© 2008 Elsevier Ltd. All rights reserved.

Keywords: FCS; Flory's random coil model; IgG; protein folding; unfolded state

Edited by C. R. Matthews

Despite its obvious importance in understanding how proteins fold, the unfolded or denatured state of proteins remains relatively unexplored.^{1,2} Recent years have thus seen an increasing number of studies focused on the conformational properties of proteins in their unfolded state.^{3–24} Of particular interest are those that assess the molecular dimensions as well as conformational dynamics of proteins under various denaturing conditions using ensemble^{11–20} or single-molecule techniques.^{25–32} All these studies, while involving a wide variety of peptides and proteins that span a large range of chain lengths (8–549 amino acids), generally support the notion that unfolded

proteins behave as self-avoiding random coils that undergo a continuous expansion with increasing concentration of denaturant, following Flory's power-law relationship (i.e., $R_G = R_0 N^{\nu}$; where R_G is the radius of gyration, R_0 is a constant determined by the persistence length of the polymer, N is the number of residues, and ν is a scaling exponent that depends on the quality of the solvent).^{11–18} In addition, several single-molecule fluorescence resonance energy transfer studies^{26,29,32} have shown that conformational transitions within an unfolded protein ensemble could occur on a range of timescales, signifying the underlying hierarchical nature of the unfolded potential well. While these previous studies provided valuable insights into the statistical properties of unfolded polypeptide chains, they focused mainly on relatively small and mostly single-domain proteins.^{12,14} To verify whether the denatured states of large multi-domain proteins exhibit similar behaviors upon chemical denaturation, here we investigate the guanidine hydrochlor-

*Corresponding author. E-mail address:
gai@sas.upenn.edu.

† L.G. and P.C. contributed equally to this work.
Abbreviations used: FCS, fluorescence correlation spectroscopy; IgG, immunoglobulin G; GdnHCl, guanidine hydrochloride; CD, circular dichroism.

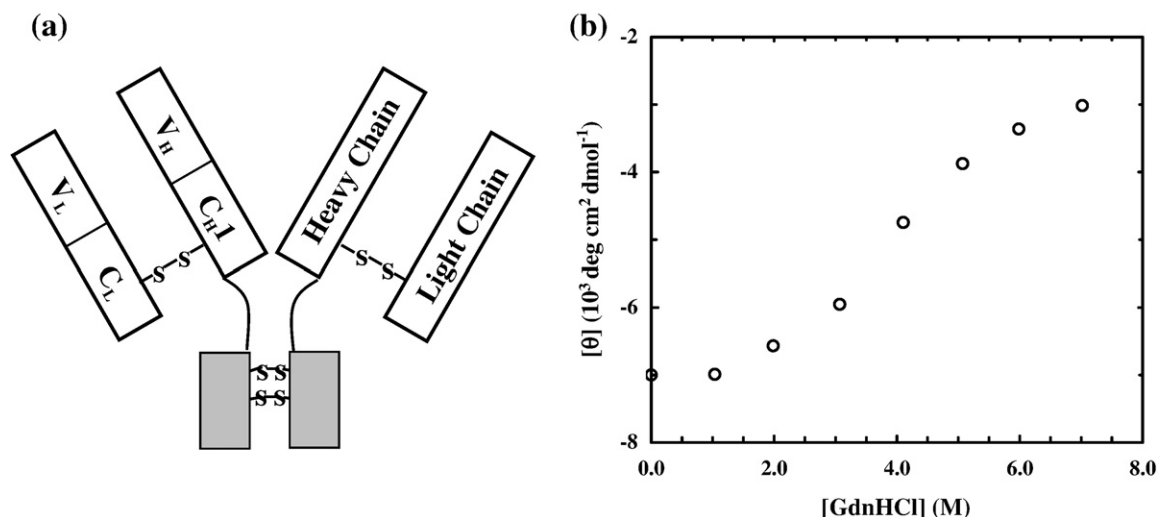


Fig. 1. (a) A representation of the $F(ab')_2$ fragment of goat IgG, showing the Y-shaped spatial disposition of the light (L) chain and part of the heavy (H) chain, linked together *via* a disulfide bridge. Each chain, as shown, is composed of a constant (C_{H1} and C_L) and a variable ($V_{H&L}$) domain, with each domain having about 110 amino acid residues. (b) Mean residue ellipticity of Alexa- $F(ab')_2$ (0.8 μ M) at 218 nm as a function of the concentration of GdnHCl (in PBS (pH 7), 100 mM NaCl). The CD data were collected on an AVIV 62DS spectrometer (Lakewood, NJ) using a 1 mm path-length quartz cell at 25 °C.

ide (GdnHCl)-induced unfolding of the $F(ab')_2$ fragment of goat anti-rabbit immunoglobulin G (IgG) and an IgG-binding protein, protein A, using fluorescence correlation spectroscopy (FCS). FCS is based on correlating fluctuations in emission intensity arising from fluorescent molecules diffusing in and out of a small confocal volume, thus providing a convenient means to measure the diffusion time and hence the molecular size of the diffusing species.^{33,34} The $F(ab')_2$ fragment (100 kDa), obtained by proteolytic cleavage of the intact goat anti-rabbit IgG, is composed of two identical Fab subunits (or arms), each consisting of four β -sheet domains.^{35,36} Two disulfide bridges bring the two Fab arms together to form a unique Y-shaped structure (Fig. 1a). Because of its distinctive structural characteristics and the prevalence of antibodies, the folding of $F(ab')_2$ as well as its constituent domains has been the subject of many studies.^{35–42} Protein A (55.5 kDa), on the other hand, is a component of the cell wall of *Staphylococcus aureus* and is known to bind to the F_C fragment of IgG.⁴³ While it also consists of multiple domains, protein A differs from $F(ab')_2$, mostly in that it lacks disulfides and is predominantly helical.

The Alexa 555-labeled IgG $F(ab')_2$ protein (referred to here as Alexa- $F(ab')_2$) studied here was purchased from Molecular Probes (Carlsbad, CA) and used without further purification. The far-UV circular dichroism (CD) spectrum of the dye-labeled $F(ab')_2$ is identical with that of unlabeled $F(ab')_2$ (data not shown), indicating that labeling does not change the integrity of the protein. Further CD studies indicate that high concentrations of GdnHCl induce Alexa- $F(ab')_2$ to unfold (Fig. 1b). Consistent with this picture, representative FCS measure-

ments[‡] show that the diffusion time of the protein molecules is distinctly lengthened in the presence of GdnHCl (Fig. 2a), a phenomenon characteristic of molecular expansion upon unfolding. More importantly, these FCS data show that the diffusion time of Alexa- $F(ab')_2$ exhibits a distinct non-monotonic dependence on the concentration of GdnHCl, a feature that has rarely been observed for other proteins. Moreover, repeated measurements reveal that the individual autocorrelation traces obtained under a given concentration of denaturant can deviate significantly from each other, indicative of a protein ensemble of varying molecular dimensions.

[‡]The FCS measurements were carried out using a confocal microscope (Nikon Eclipse TE 300) setup equipped with an oil immersion objective (N.A.=1.3) and a 50 μ m confocal pinhole.^{44,45} Excitation of the Alexa 555-labeled protein samples (3–5 nM) was accomplished by the 514 nm line of an argon ion laser (\sim 100 μ W before entering the microscope), and the resultant fluorescence was split equally by a nonpolarizing beamsplitter (Newport, CA) and detected by two avalanche photodiodes (Perkin Elmer, NJ) using an integration time of 1 μ s. Correlating the fluorescence signals in the cross-correlation mode was accomplished by a Flex 03-LQ-01 correlator card (Correlator.com, NJ) for a duration of 150 s. It is known that high concentrations of GdnHCl and urea increase the confocal volume (due to refractive index mismatch) and the viscosity of the solution, both lengthening the apparent diffusion time. Thus, all the τ_D values obtained from FCS measurements involving denaturants were “corrected” to yield the reported values following common practice,^{25,30} namely, by calibrating the aforementioned effects using the diffusion time of a standard (R6G in the current case) measured under the same solution conditions.

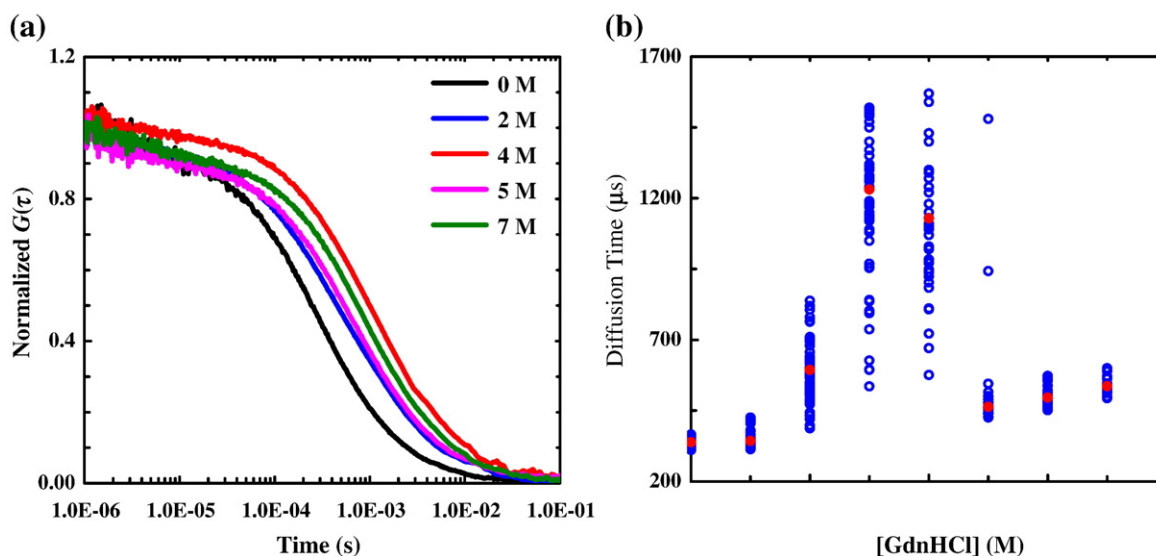


Fig. 2. (a) Representative autocorrelation traces of Alexa-F(ab')₂ measured at different concentrations of GdnHCl, as indicated. Fitting these FCS data to Eq. (1) yields the following diffusion times: $\tau_D = 337 \mu\text{s}$ for 0 M GdnHCl, $\tau_D = 595 \mu\text{s}$ for 2 M GdnHCl, $\tau_{D1} = 544 \mu\text{s}$ and $\tau_{D2} = 1300 \mu\text{s}$ for 4 M GdnHCl, $\tau_D = 462 \mu\text{s}$ for 5 M GdnHCl, and $\tau_D = 527 \mu\text{s}$ for 7 M GdnHCl. These results show that the characteristic diffusion time of F(ab')₂ is nonlinearly dependent on [GdnHCl]. (b) The corrected (see the text) diffusion times (blue open circles) of Alexa-F(ab')₂ obtained at different concentrations of GdnHCl. Also shown (red circles) are the respective averages.

In order to provide a more quantitative picture regarding how the molecular diffusion of the IgG F(ab')₂ fragment changes as a function of [GdnHCl], a minimum of 30 autocorrelation traces were collected under each denaturation condition and analyzed according to the following equation:³⁴

$$G(\tau) = \left(\sum_{i=1}^n \frac{1}{N} \left(\frac{1}{1 + \frac{\tau}{\tau_D^i}} \right) \left(\frac{1}{1 + \frac{\tau}{\omega^2 \tau_D^i}} \right)^{1/2} \right) \times \left(1 - T + T \cdot e^{-\left(\frac{\tau}{\tau_{\text{triplet}}}\right)} \right) \quad (1)$$

where τ_D^i represents the characteristic diffusion time of species i , ω refers to the axial to lateral dimension ratio of the confocal volume element, N is the number of fluorescent molecules in the confocal volume, τ_{triplet} is the triplet lifetime of the fluorophore and T is the corresponding triplet amplitude. For Alexa-F(ab')₂ in 100 mM PBS at pH 7, all the autocorrelation traces can be well described by Eq. (1) with $n=1$ and τ_D of $340 \pm 30 \mu\text{s}$. Similarly, for [GdnHCl]=1 M, 2 M, 5 M, 6 M, and 7 M, the respective autocorrelation traces can be modeled adequately by Eq. (1) with $n=1$. However, in order to fit those autocorrelation traces obtained in 3 M or 4 M GdnHCl, two diffusion components (i.e., $n=2$ in Eq. (1)) have to be invoked. In this regard, it is worth pointing out that FCS is commonly considered a single-molecule technique based on the fact that most of the recorded fluorescence bursts arise primarily from individual molecules traversing the confocal volume element. However, a typical FCS measurement involves the collection of an appreciable number of such bursts arising from many probe

molecules diffusing in and out of the excitation volume. Hence, the resultant autocorrelation trace is in fact a weighted average of the diffusion profiles of all the individual molecules contributing to the aforementioned fluctuations in fluorescence.²⁵ While in principle, one should be able to extract the characteristic diffusion time of each and every molecule contributing to the autocorrelation trace, both simulation and experimental studies have shown that in order to differentiate between two species using this technique, their diffusion times have to differ by at least a factor of 1.6.⁴⁶ In other words, for a group of molecules whose diffusion times are not significantly different, an FCS measurement would result in an autocorrelation trace that can be well described by Eq. (1) with $n=1$ and yield a τ_D value corresponding to the weighted average of the diffusion times of all the contributing molecules. On the other hand, for a group of molecules that exhibit marked differences in their diffusion times, two or more diffusion components will be required to fit the experimentally measured autocorrelation traces reliably, depending on the number of diffusion events (or the total observation time) as well as the separations in their respective diffusion timescales.²⁵

For the reasons discussed above, it is clear that a single FCS experiment might fail to reveal the diffusion heterogeneity intrinsic to an unfolded protein ensemble. However, such heterogeneity may be unmasked through a series of repeated FCS measurements, as demonstrated in the current case (see below), provided that the underlying reconfiguration times among different conformations are slower than their respective transit times through the confocal volume. This is because, despite the fact that

many molecules contribute to each individual FCS trace, the actual number is nevertheless very small compared to the total number of fluorescent molecules in the sample solution. Thus, a set of individual FCS measurements would yield τ_D values that statistically fluctuate around a mean value, determined by the intrinsic size distribution of the protein ensemble under investigation.

As shown (Fig. 2b), the characteristic diffusion times of Alexa-F(ab')₂ not only show a complex dependence on [GdnHCl] but also vary quite considerably among individual measurements. In particular, three key observations merit elaboration. First, at an intermediate concentration of GdnHCl (i.e., 2–5 M) the diffusion of Alexa-F(ab')₂ is characterized by a range of τ_D values with a standard deviation much larger than that arising from the uncertainties commonly associated with FCS experiments.⁴⁷ For example, the data obtained at 2 M GdnHCl yield a mean diffusion time of 600 μ s with a deviation of \sim 200 μ s around the mean. The latter is significantly greater than that (i.e., 30 μ s) observed for the protein under native conditions. In addition, for 3 M or 4 M GdnHCl, the recovered diffusion times spread over an even larger time window. Hence, as discussed above, these results indicate that under such conditions the Alexa-F(ab')₂ molecules sample a large set of conformations that are distinguishable by their respective diffusion characteristics. Furthermore, these results imply that the interconversion rates among different conformations are slow enough that the hydrodynamic radius of most molecules remains unchanged while traversing the confocal volume,²⁵ thus allowing the recovery of distinctly different diffusion times. Consistent with this picture, it has been shown that Fab unfolds very slowly.^{36,40,41} In addition, these results are in accord with the fact that each Fab arm contains 23 proline residues, the isomerization of which would definitely slow the interconversion rates among different denatured conformations. Second, increasing the GdnHCl concentration from 0 to 4 M leads to a significant increase in the average diffusion time of the protein, from 340 μ s to \sim 1.2 ms. This indicates that, on average, the molecular dimension of F(ab')₂ in 4 M GdnHCl is significantly larger than that of the native F(ab')₂. Considering the fact that a large number of proteins have now been shown to expand only modestly upon denaturation,^{14,17,18} this result is quite surprising and unexpected. The final, and perhaps the most intriguing observation is that a further increase in [GdnHCl] from 4 M to 6 M or 7 M results in a considerable compaction of the protein molecules, as judged by the significant decrease in the average diffusion times under these conditions.

Taken together, these results indicate that the GdnHCl-induced denaturation of this large, multi-domain, multi-subunit protein, as monitored by the change in diffusion times (τ_D) and hence the associated hydrodynamic radii (discussed below) as a function of [GdnHCl], is markedly different from the commonly observed continuous expansion

behavior.^{26,27,30} To further probe into this aspect, and for the purpose of comparison, we have performed similar FCS measurements on protein A, a 508 residue protein composed of five helical domains. Both CD (data not shown) and FCS measurements (Fig. 3) corroborate each other in that protein A unfolds progressively with increasing concentration of denaturant. However, in marked contrast to what has been observed for F(ab')₂, the molecular dimension of this IgG-binding protein shows a continuous and very modest expansion upon chemical denaturation, as suggested by Flory's random-coil model.⁴⁸

The hydrodynamic radius (R_h) of a spherical diffusing species is related to τ_D through the following equation:^{24,25}

$$\tau_D = 6\pi\eta R_h r_0^2 / 4k_B T \quad (2)$$

where r_0 is the lateral dimension of the confocal volume element (\sim 0.26 μ m in the current case), η represents the viscosity of the solution, k_B is Boltzmann's constant and T is the absolute temperature. Using Eq. (2) and the measured τ_D of 340 ± 30 μ s, the hydrodynamic radius of F(ab')₂ in its folded state was calculated to be 44 ± 4 \AA . This value is very similar to that (44.8 \AA) determined by other techniques for the same fragment of IgG in buffer,^{49,50} further validating the current method. Similarly, using the average τ_D value obtained in 7 M GdnHCl, we have estimated the hydrodynamic radius of the denatured F(ab')₂ to be \sim 70 \AA . This result appears to be consistent with the notion that the hydrodynamic radius of the highly denatured ensemble of proteins follows Flory's scaling law,^{11–18} $R_h = 2.21 N^{0.57}$, which predicts an R_h of 113 \AA for the highly denatured F(ab')₂ molecules. The apparent difference is likely due to the fact that there are 12 disulfides in F(ab')₂, which can certainly exert conformational constraints.

On the other hand, based on the same premise (presence of disulfide bonds), the observation of the

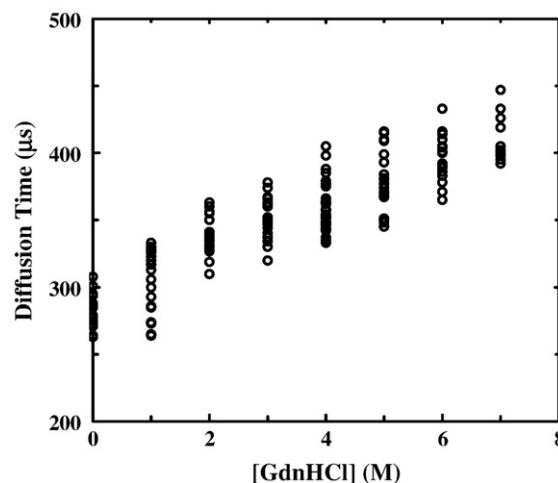


Fig. 3. The corrected (see the text) diffusion times of protein A obtained at different concentrations of GdnHCl.

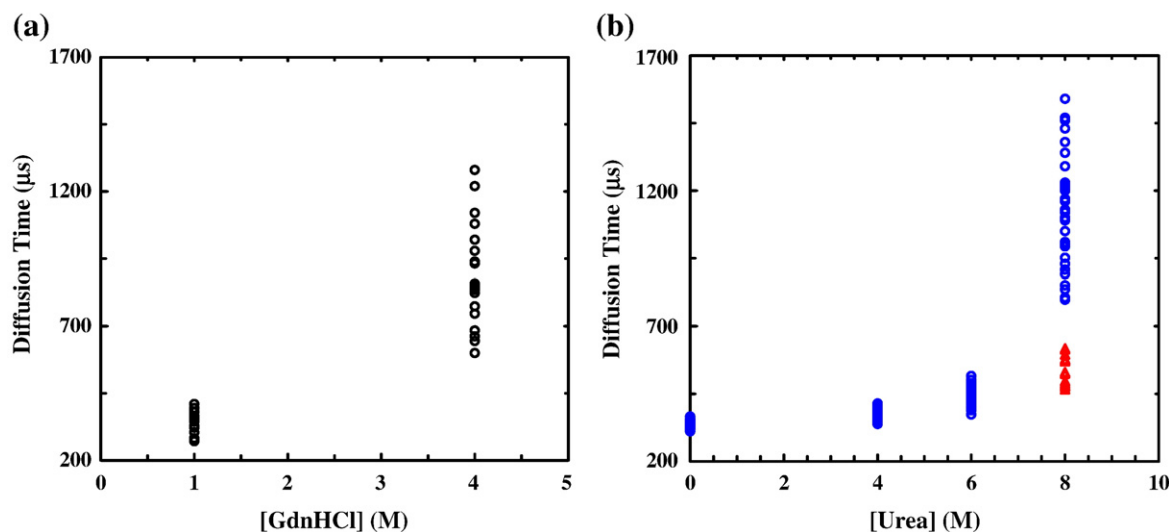


Fig. 4. (a) The corrected (see the text) diffusion times of Alexa-F(ab')₂ obtained at 4 M and 1 M GdnHCl. The 1 M GdnHCl sample was prepared by dilution of the 4 M GdnHCl protein sample used to generate the data presented here. These results indicate that the denaturation is reversible under the current experimental conditions. (b) The corrected (see the text) diffusion times of Alexa-F(ab')₂ obtained in urea (blue) and 2 M NaCl-urea (red) solutions.

very slow-moving species at 3 M and 4 M GdnHCl is indeed quite unexpected. For example, the average τ_D is ~ 1.2 ms under these conditions, which gives rise to an R_h value of ~ 161 Å according to Eq. (2), corresponding to ~ 3.6 times that of the folded conformation. Since protein aggregation can also yield diffusing species with a prolonged diffusion time, special precautions and measures have been taken to prevent formation of such aggregates. Firstly, the coverslips used for the FCS measurements were surface-passivated with either BSA (Pierce Chemicals, Rockford, IL) or PEG-silane (Gelest Inc., Morrisville, PA) to minimize the tendency of adhesion and surface-induced aggregation of the protein molecules under investigation. Secondly, the nanomolar Alexa-F(ab')₂ samples used in the FCS experiments were prepared by directly diluting the stock protein solution (10 μM) from Molecular Probes by the desired denaturant solution so as to minimize aggregate formation under denaturing conditions. In addition, all the fluorescence burst profiles were scrutinized carefully and were found to have very similar brightness, suggesting that they arise from monomeric Alexa-F(ab')₂ molecules as aggregates would appear brighter due to the increased number of fluorophores per diffusing species.⁵¹ However, to provide more direct evidence that the protein molecules under current experimental conditions are predominantly monomeric, we have examined the reversibility of the GdnHCl-induced denaturation of Alexa-F(ab')₂. As shown (Fig. 4a), the distribution of the diffusion times of Alexa-F(ab')₂ is reversible upon dilution of the denaturant after unfolding (e.g., from 4 M to 1 M). Since protein aggregation is usually irreversible, these results suggest strongly that the slow-moving species observed at intermediate concentrations of GdnHCl do not

correspond to aggregates of the labeled F(ab')₂ fragments. In addition, fast protein liquid chromatography (FPLC) measurements[§] provide further evidence that even at a concentration of 1.5 μM, Alexa-F(ab')₂ exists as monomer in 4 M GdnHCl.

Tentatively, we hypothesize that electrostatic repulsion is the dominant factor leading to the formation of such a highly expanded F(ab')₂ ensemble at intermediate concentration of denaturant. To provide experimental evidence supporting this hypothesis, we have further studied the urea-induced denaturation of Alexa-F(ab')₂ using FCS. Urea, another commonly used denaturant in protein unfolding studies, differs from GdnHCl mostly in that the latter is a salt and hence can not only disrupt hydrophobic interactions but also greatly affect electrostatic forces.⁵² As shown (Fig. 4b), in 8 M urea the distribution of the diffusion times of Alexa-F(ab')₂ is quite similar to that observed in 4 M GdnHCl, showing the presence of an ensemble of highly expanded species. However, addition of 2 M NaCl to the 8 M urea sample leads to a significant reduction in the average diffusion times, indicative of compaction in molecular dimensions. Thus, these results suggest that electrostatic interactions play an important role in defining the final molecular

[§]FPLC measurements were carried out on an Akta FPLC system (GE Healthcare). The column was calibrated by using high molecular mass standards as described in the manufacturer's protocol. Alexa-F(ab')₂ (1.5 μM in 4 M GdnHCl at pH 7) was incubated overnight. This sample was then passed through a Superdex S200 column under the same denaturing conditions (i.e., in the presence of 4 M GdnHCl). The elution trace, monitored by measuring the absorbance at 280 nm, showed a single peak at 10.3 mL, which corresponds to the molecular mass of monomeric Alexa-F(ab')₂ based on the calibration.

dimensions of the denatured $F(ab')_2$ molecules. In other words, the complex dependence of the diffusion time (and hence the hydrodynamic radius) of $F(ab')_2$ as a function of $[GdnHCl]$ results from two opposing effects: (i) significant swelling of the protein due to unusual electrostatic repulsions upon unfolding, which dominates at relatively low concentrations of denaturant, and (ii) electrostatic shielding provided by the $GdnHCl$ salt, which becomes more pronounced at high concentrations of denaturant. Hence, with increasing $[GdnHCl]$, $F(ab')_2$ first expands due to unfolding and then undergoes a transition leading to the formation of a more compact conformational ensemble owing to the increased screening that diminishes the charge repulsions. Consistent with this picture, $F(ab')_2$ carries a net charge of +20 at neutral pH, and this net charge is distributed evenly among the four chains. In particular, the V_L (V_H) domain carries a net charge of +6 (+3). Because the V_H and V_L domains are in close proximity, these net charges may play an important role in determining the size of the unfolded state of $F(ab')_2$. Additionally, the disulfides in $F(ab')_2$ may also have a subtle but important role in generating the more extended conformational ensemble because they eliminate a large number of feasible conformations.

While the Flory's model treats unfolded proteins as polymers consisting of uncorrelated monomers, such a mean-field treatment nevertheless yields a scaling law (i.e., $R_G = R_0 N^\nu$), arising from the repulsive excluded volume (EV) effects, that fits a large number of experimental data.^{12,14} Thus, the observation here of an overly expanded $F(ab')_2$ ensemble is indeed surprising. However, it is consistent with the notion that electrostatic interactions can influence the radius of gyration of proteins. For instance, it has been shown that several intrinsically unfolded proteins (e.g., γ -synuclein and prothymosin- α) in water have dimensions far beyond those predicted on the basis of random-coil statistics^{12,14} (in one case by as much as twofold) due to their unusually high density of charges. Also, in a related study,⁵³ Thirumalai and co-workers have shown that certain ribosomal proteins show considerably larger R_G values than predicted by Flory's scaling law, due to the long, positively charged, unstructured chains in the tail region of the protein. Moreover, charge-charge interactions have been shown to play a distinct role in the unfolded states of proteins,⁵⁴ such as barstar,⁵⁵ cytochrome c ,^{56,57} staphylococcal nuclease,^{56,58} and ribonuclease Sa.⁵⁹ Furthermore, force-quench refolding simulations of the I27 immunoglobulin domain of the muscle protein titin indicate ~ 6 -fold reduction in the radius of gyration when the molecule refolds from its unfolded (stretched) state,⁶⁰ suggesting that it is possible to generate an expanded and thus slowly diffusing species.

In summary, using FCS we have examined the size distribution of two multi-domain proteins, protein A and the $F(ab')_2$ fragment of IgG as a function of the concentration of $GdnHCl$. $F(ab')_2$ is a predomi-

nantly β -sheet protein, whereas protein A is composed of mostly α -helices. Our results show that while $GdnHCl$ induces protein A to expand in a gradual manner, consistent with the so-called continuous expansion model, the effect of $GdnHCl$ on the molecular dimension of $F(ab')_2$ is much more complicated. In particular, at intermediate concentrations of denaturant, the $F(ab')_2$ molecules adopt a highly expanded form with a molecular dimension exceeding the value predicted by Flory's model. On the other hand, at high concentrations of denaturant, the unfolded protein ensemble undergoes a significant compaction. Further denaturation experiments carried out with urea in the presence of high concentrations of salt appear to indicate that electrostatic repulsive interactions play an important role in giving rise to the unusual expansion of the $F(ab')_2$ fragment of IgG upon unfolding. Thus, these results together suggest that the nature and extent of specific interactions in a particular protein might lead to significant deviation from the commonly encountered continuous and gradual expansion model of protein unfolding.

Acknowledgements

We gratefully acknowledge financial support from the National Institutes of Health (GM-065978 and RR-01348) and the National Science Foundation (DMR05-20020). J.M.G. is a trainee of the NIH Structural Biology Training Program at Penn. We thank Dr Dmochowski's group for assistance with the FPLC measurement.

References

1. Dill, K. A. & Shortle, D. (1991). Denatured states of proteins. *Annu. Rev. Biochem.* **60**, 795–825.
2. Smith, L. J., Fiebig, K. M., Schwalbe, H. & Dobson, C. M. (1996). The concept of a random coil. Residual structure in peptides and unfolded proteins. *Fold. Des.* **1**, R95–R106.
3. Wong, K. B., Clarke, J., Bond, C. J., Neira, J. L., Freund, S. M. V., Fersht, A. R. & Daggett, V. (2000). Towards a complete description of the structural and dynamic properties of the denatured state of barnase and the role of residual structure in folding. *J. Mol. Biol.* **296**, 1257–1282.
4. Dyson, J. H. & Wright, P. E. (2002). Insights into the structure and dynamics of unfolded proteins from nuclear magnetic resonance. *Adv. Protein Chem.* **62**, 311–340.
5. Zagrovic, B., Snow, C. D., Khaliq, S., Shirts, M. R. & Pande, V. S. (2002). Native-like mean structure in the unfolded ensemble of small proteins. *J. Mol. Biol.* **323**, 153–164.
6. Tang, Y. F., Rigotti, D. J., Fairman, R. & Raleigh, D. P. (2004). Peptide models provide evidence for significant structure in the denatured state of a rapidly folding protein: The villin headpiece subdomain. *Biochemistry*, **43**, 3264–3272.
7. Tucker, M. J., Oyola, R. & Gai, F. (2005). Conformational

- distribution of a 14-residue peptide in solution: A fluorescence resonance energy transfer study. *J. Phys. Chem. B*, **109**, 4788–4795.
8. Bernado, P., Blanchard, L., Timmins, P., Marion, D., Ruigrok, R. W. H. & Blackledge, M. (2005). A structural model for unfolded proteins from residual dipolar couplings and small-angle X-ray scattering. *Proc. Natl Acad. Sci. USA*, **102**, 17002–17007.
 9. Bilsel, O. & Matthews, C. R. (2006). Molecular dimensions and their distributions in early folding intermediates. *Curr. Opin. Struct. Biol.* **16**, 86–93.
 10. Mittag, T. & Forman-Kay, J. D. (2007). Atomic-level characterization of disordered protein ensembles. *Curr. Opin. Struct. Biol.* **17**, 3–14.
 11. Wilkins, D. K., Grimshaw, S. B., Receveur, V., Dobson, C. M., Jones, J. A. & Smith, L. J. (1999). Hydrodynamic radii of native and denatured proteins measured by pulse field gradient NMR techniques. *Biochemistry*, **38**, 16424–16431.
 12. Millet, I. S., Doniach, S. & Plaxco, K. W. (2002). Toward a taxonomy of the denatured state: Small angle scattering studies of unfolded proteins. *Adv. Protein Chem.* **62**, 241–262.
 13. Choy, W.-Y., Mulder, F. A. A., Crowhurst, K. A., Muhandiram, D. R., Millett, I. S., Doniach, S. *et al.* (2002). Distribution of molecular size within an unfolded state ensemble using small-angle X-ray scattering and pulse field gradient NMR techniques. *J. Mol. Biol.* **316**, 101–112.
 14. Kohn, J. E., Millett, I. S., Jacob, J., Zagrovic, B., Dillon, T. M., Cingel, N. *et al.* (2004). Random-coil behavior and the dimensions of chemically unfolded proteins. *Proc. Natl Acad. Sci. USA*, **101**, 12491–12496.
 15. Fitzkee, N. C. & Rose, G. D. (2004). Reassessing random-coil statistics in unfolded proteins. *Proc. Natl Acad. Sci. USA*, **101**, 12497–12502.
 16. Jha, A. K., Colubri, A., Freed, K. F. & Sosnick, T. R. (2005). Statistical coil model of the unfolded state: Resolving the reconciliation problem. *Proc. Natl Acad. Sci. USA*, **102**, 13099–13104.
 17. Jacob, J., Dothager, R. S., Thiyagarajan, P. & Sosnick, T. R. (2007). Fully reduced ribonuclease A does not expand at high denaturant concentration or temperature. *J. Mol. Biol.* **367**, 609–615.
 18. Wang, Z., Plaxco, K. W. & Makarov, D. E. (2007). Influence of local and residual structures on the scaling behavior and dimensions of unfolded proteins. *Biopolymers*, **86**, 321–328.
 19. Lipfert, J. & Doniach, S. (2007). Small-angle X-ray scattering from RNA, proteins, and protein complexes. *Annu. Rev. Biophys. Biomol. Struct.* **36**, 307–327.
 20. Zhou, H. X. (2002). Dimensions of denatured protein chains from hydrodynamic data. *J. Phys. Chem. B*, **106**, 5769–5775.
 21. Goldenberg, D. P. (2003). Computational simulation of the statistical properties of unfolded proteins. *J. Mol. Biol.* **326**, 1615–1633.
 22. Dima, R. I. & Thirumalai, D. (2004). Asymmetry in the shapes of folded and denatured states of proteins. *J. Phys. Chem. B*, **108**, 6564–6570.
 23. Ding, F., Jha, R. K. & Dokholyan, N. V. (2005). Scaling behavior and structure of denatured proteins. *Structure*, **13**, 1047–1054.
 24. Tran, H. T. & Pappu, R. V. (2006). Toward an accurate theoretical framework for describing ensembles for proteins under strongly denaturing conditions. *Biophys. J.* **91**, 1868–1886.
 25. Frieden, C., Chattopadhyay, K. & Elson, E. L. (2002). What fluorescence correlation spectroscopy can tell us about unfolded proteins. *Adv. Protein Chem.* **62**, 91–110.
 26. Kuzmenkina, E. V., Heyes, C. D. & Nienhaus, G. U. (2005). Single-molecule Förster resonance energy transfer study of protein dynamics under denaturing conditions. *Proc. Natl Acad. Sci. USA*, **102**, 15471–15476.
 27. Chattopadhyay, K., Saffarian, S., Elson, E. L. & Frieden, C. (2005). Measuring unfolding of proteins in the presence of denaturant using fluorescence correlation spectroscopy. *Biophys. J.* **88**, 1413–1422.
 28. McCarney, E. R., Werner, J. H., Bernstein, S. L., Ruczinski, I., Makarov, D. E., Goodwin, P. M. & Plaxco, K. W. (2005). Site-specific dimensions across a highly denatured protein; a single molecule study. *J. Mol. Biol.* **352**, 672–682.
 29. Slaughter, B. D., Unruh, J. R., Price, E. S., Huynh, J. L., Urbauer, R. J. B. & Johnson, C. K. (2005). Sampling unfolding intermediates in calmodulin by single-molecule spectroscopy. *J. Am. Chem. Soc.* **127**, 12107–12114.
 30. Sherman, E. & Haran, G. (2006). Coil-globule transition in the denatured state of a small protein. *Proc. Natl Acad. Sci. USA*, **103**, 11539–11543.
 31. Chen, H. M., Rhoades, E., Butler, J. S., Loh, S. N. & Webb, W. W. (2007). Dynamics of equilibrium structural fluctuations of apomyoglobin measured by fluorescence correlation spectroscopy. *Proc. Natl Acad. Sci. USA*, **104**, 10459–10464.
 32. Merchant, K. A., Best, R. B., Louis, J. M., Gopich, I. V. & Eaton, W. A. (2007). Characterizing the unfolded states of proteins using single-molecule FRET spectroscopy and molecular simulations. *Proc. Natl Acad. Sci. USA*, **104**, 1528–1533.
 33. Magde, D., Elson, E. L. & Webb, W. W. (1974). Fluorescence correlation spectroscopy. 2. Experimental realization. *Biopolymers*, **13**, 29–61.
 34. Hausteiner, E. & Schwiile, P. (2007). Fluorescence correlations spectroscopy: novel variations of an established technique. *Annu. Rev. Biophys. Biomol. Struct.* **36**, 151–169.
 35. Lilie, H. & Buchner, J. (1995). Domain interactions stabilize the alternatively folded state of an antibody Fab fragment. *FEBS Lett.* **362**, 43–46.
 36. Lilie, H. (1997). Folding of the Fab fragment within the intact antibody. *FEBS Lett.* **417**, 239–242.
 37. Goto, Y. & Hamaguchi, K. (1982). Unfolding and refolding of the constant fragment of the immunoglobulin light chain. *J. Mol. Biol.* **156**, 891–910.
 38. Goto, Y. & Hamaguchi, K. (1982). Unfolding and refolding of the constant fragment of the immunoglobulin light chain — kinetic role of the intrachain disulfide bond. *J. Mol. Biol.* **156**, 911–926.
 39. Bork, P., Holm, L. & Sander, C. (1994). The immunoglobulin fold — structural classification, sequence patterns and common core. *J. Mol. Biol.* **242**, 309–320.
 40. Lilie, H., Rudolph, R. & Buchner, J. (1995). Association of antibody chains at different stages of folding: prolyl isomerization occurs after formation of quaternary structure. *J. Mol. Biol.* **248**, 190–201.
 41. Rothlisberger, D., Honegger, A. & Pluckthun, A. (2005). Domain interactions in the Fab fragment: a comparative evaluation of the single-chain Fv and Fab format engineered with variable domains of different stability. *J. Mol. Biol.* **347**, 773–789.
 42. Feige, M. J., Hagn, F., Esser, J., Kessler, H. & Buchner, J. (2007). Influence of the internal disulfide bridge on the folding pathway of the C–L antibody domain. *J. Mol. Biol.* **365**, 1232–1244.
 43. Moks, T., Abrahamsen, L., Nilsson, B., Hellman, U.,

- Sjoquist, J. & Uhlen, M. (1986). Staphylococcal protein A consists of five IgG-binding domains. *Eur. J. Biochem.* **156**, 637–643.
44. Purkayastha, P., Klemke, J. W., Lavender, S., Oyola, R., Cooperman, B. S. & Gai, F. (2006). $\alpha(1)$ -Antitrypsin polymerization: A fluorescence correlation spectroscopic study. *Biochemistry*, **44**, 2642–2649.
45. Chowdhury, P., Wang, W., Lavender, S., Bunagan, M. R., Klemke, J. W., Tang, J. *et al.* (2007). Fluorescence correlation spectroscopic study of serpin depolymerization by computationally designed peptides. *J. Mol. Biol.* **369**, 462–473.
46. Meseth, U., Wohland, T., Rigler, R. & Vogel, H. (1999). Resolution of fluorescence correlation measurements. *Biophys. J.* **76**, 1619–1631.
47. Wohland, T., Rigler, R. & Vogel, H. (2001). The standard deviation in fluorescence correlation spectroscopy. *Biophys. J.* **80**, 2987–2999.
48. Flory, P. J. (1949). The configuration of real polymer chains. *J. Chem. Phys.* **17**, 303–310.
49. Starr, T. E. & Thompson, N. L. (2002). Local diffusion and concentration of IgG near planar membranes: Measurement by total internal reflection with fluorescence correlation spectroscopy. *J. Phys. Chem. B*, **106**, 2365–2371.
50. Armstrong, J. K., Wenby, R. B., Meiselman, H. J. & Fisher, T. C. (2004). The hydrodynamic radii of macromolecules and their effect on red blood cell aggregation. *Biophys. J.* **87**, 4259–4270.
51. Crick, S. L., Jayaraman, M., Frieden, C., Wetzel, R. & Pappu, R. V. (2006). Fluorescence correlation spectroscopy shows that monomeric polyglutamine molecules form collapsed structures in aqueous solutions. *Proc. Natl Acad. Sci. USA*, **103**, 16764–16769.
52. Makhatadze, G. I. & Privalov, P. L. (1992). Protein interactions with urea and guanidium chloride — a calorimetric study. *J. Mol. Biol.* **226**, 491–505.
53. Changbong, H., Dima, R. I. & Thirumalai, D. (2006). Size, shape, and flexibility of RNA structures. *J. Chem. Phys.* **125**, 194905.
54. Zhou, H. X. (2002). A Gaussian-chain model for treating residual charge-charge interactions in the unfolded state of proteins. *Proc. Natl Acad. Sci. USA*, **99**, 3569–3574.
55. Hofmann, H., Golbik, R. P., Ott, M., Hübner, C. G. & Ulbrich-Hofmann, R. (2008). Coulomb forces control the density of the collapsed unfolded state of barstar. *J. Mol. Biol.* **376**, 597–605.
56. Kundrotas, P. K. & Karshikoff, A. (2003). Effects of charge-charge interactions on dimensions of unfolded proteins: A monte carlo study. *J. Chem. Phys.* **119**, 3574–3581.
57. Segel, D. J., Fink, A. L., Hodgson, K. O. & Doniach, S. (1998). Protein denaturation: A small-angle X-ray scattering study of the ensemble of unfolded states of cytochrome c. *Biochemistry*, **37**, 12443–12451.
58. Panick, G., Malessa, R., Winter, R., Rapp, G., Frye, K. J. & Royer, C. A. (1998). Structural characterization of the pressure-denatured state and unfolding/refolding kinetics of staphylococcal nuclease by synchrotron small-angle X-ray scattering and Fourier-transform infrared spectroscopy. *J. Mol. Biol.* **275**, 389–402.
59. Pace, C. N., Alston, R. W. & Shaw, K. L. (2000). Charge-charge interactions influence the denatured state ensemble and contribute to protein stability. *Protein Sci.* **9**, 1395–1398.
60. Li, M. S., Hu, C. K., Klimov, D. K. & Thirumalai, D. (2006). Multiple stepwise refolding of immunoglobulin domain I27 upon force quench depends on initial conditions. *Proc. Natl Acad. Sci. USA*, **103**, 93–98.